IOPscience iopscience.iop.org

Home Search Collections Journals About Contact us My IOPscience

The conduction band and selection rules for interband optical transitions in strained $Ge_{1-x}Si_x/Ge$ and $Ge_{1-x}Si_x/Si$ heterostructures

This article has been downloaded from IOPscience. Please scroll down to see the full text article.

1997 J. Phys.: Condens. Matter 9 4841

(http://iopscience.iop.org/0953-8984/9/23/008)

View the table of contents for this issue, or go to the journal homepage for more

Download details:
IP Address: 171.66.16.151
The article was downloaded on 12/05/2010 at 23:09

Please note that terms and conditions apply.

J. Phys.: Condens. Matter **9** (1997) 4841–4852. Printed in the UK PII: S0953-8984(97)80290-1

The conduction band and selection rules for interband optical transitions in strained $Ge_{1-x}Si_x$/Ge and $Ge_{1-x}Si_x$/Si heterostructures

V Ya Aleshkin and N A Bekin

Institute for the Physics of Microstructures of the Russian Academy of Sciences, 603600, Nizhny Novgorod GSP-105, Russia†

Received 12 December 1996, in final form 7 March 1997

Abstract. The conduction-band alignments of $Ge_{1-x}Si_x$/Ge and $Ge_{1-x}Si_x$/Si heterostructures grown on (111) and (001) crystallographic planes, respectively, are analysed. We have obtained the selection rules for interband dipole optical transitions in the heterostructures, and discussed the possibilities for specifying the types of the lowest conduction-band minima. We show that this can be done by, for example, exploring the polarization of different phonon-assisted band-edge optical transitions.

The conduction-band minima may be at different L or Δ points of the Brillouin zone, depending on the structure parameters. Although bulk Ge, Si, and their alloy are indirect-gap semiconductors, the heterostructures $Ge_{1-x}Si_x$/Ge and $Ge_{1-x}Si_x$/Si can have a direct band gap. We found the parameter regions where type-I and type-II band alignment were realized, and those where the band gap was direct in quantum well (QW) structures. It is shown that in direct-gap QW structures grown on (001) planes, direct interband optical transitions between the nearest electron and hole subbands are allowed, but the same transitions are forbidden for direct-gap structures grown on (111) planes.

1. Introduction

As silicon is extensively used in electric circuits, Si-based materials are of great research interest. In particular, $Ge_{1-x}Si_x$/Ge and $Ge_{1-x}Si_x$/Si heterostructures have been intensively investigated in the last few years.

The lattice constants of Ge and Si are mismatched by 4%, and either one or both of the materials in the heterostructures are strained. In the pseudomorphic heterostructures, the potential wells for holes are known to be in layers with a smaller Si fraction, for a wide range of strain and for any orientation of the heterojunction plane (see, for example, [1–5]). However, there is no clear understanding about the conduction bands of these heterostructures over a broad range of their parameters, because there are several conduction-band minima both in the $Ge_{1-x}Si_x$ alloy and in the pure Si and Ge, whose position depends upon strain and x. Even for the intensively investigated $Ge_{1-x}Si_x$/Si heterostructures matched to unstrained Si, there are contradictory data regarding the type of band alignment for x near 1 [1, 6, 7].

In this work we analyse the conduction bands of $Ge_{1-x}Si_x$/Ge and $Ge_{1-x}Si_x$/Si heterostructures grown on (111) and (001) crystallographic planes, respectively. Our investigation

† Fax: (8312) 675553; e-mail: aleshkin@ipm.sci-nnov.ru.

0953-8984/97/234841+12$19.50 © 1997 IOP Publishing Ltd

is based on *ab initio* calculations made by Van de Walle and Martin [4], and by Rieger and Vogl [5]. We have obtained the selection rules for interband dipole optical transitions in the heterostructures, and we discuss the possibilities for specifying the type of the lowest conduction-band minima by using the selection rules. We show that this can be done by, for example, exploring the polarization of different phonon-assisted band-edge optical transitions.

The band alignment of a heterojunction is found to be type-I or type-II alignment, depending on the heterostructure parameters. The conduction-band minima may be at different L or Δ points of the Brillouin zone. Although bulk Ge, Si, and their alloy are indirect-gap semiconductors, the $Ge_{1-x}Si_x$/Ge and $Ge_{1-x}Si_x$/Si heterostructures can have a direct band gap [8]. The latter is realized if the conduction-band bottom is in the valley, with the minimum quasi-momentum being perpendicular to the heterointerfaces. As this takes place, in the heterostructures with thin layers an electron easily loses the corresponding quasi-momentum by collision with heterointerfaces. This manifests itself in the fact that the Brillouin zone of a quantum well (QW) system becomes a two-dimensional one. The quasi-momentum directed perpendicularly to the heterojunction plane is absent in such a Brillouin zone. We have found the parameter regions where type-I and type-II band alignments are realized, and those where the band gap is direct, in QW structures. It is shown that in direct-gap (001) structures, direct interband optical transitions between the nearest electron and hole subbands are allowed, but the same transitions are forbidden for direct-gap (111) structures. Note that in short-period superlattices, a band gap can become direct as a result of a folding effect [9].

In section 2, the conduction band of the $Ge_{1-x}Si_x$/Ge and $Ge_{1-x}Si_x$/Si heterostructures is investigated. Our results are compared with some experimental data. Selection rules and the related possible methods of experimental exploration of the conduction band are presented in sections 3 and 4 for $Ge_{1-x}Si_x$/Ge and $Ge_{1-x}Si_x$/Si heterostructures, respectively.

2. The conduction bands of (111) $Ge_{1-x}Si_x$/Ge and (001) $Ge_{1-x}Si_x$/Si heterostructures

The valence-band discontinuities in $Ge_{1-x}Si_x$/Ge and $Ge_{1-x}Si_x$/Si heterostructures were derived using the *ab initio* pseudopotentials given in [4, 5]. Using these values, one can easily define the energy of the conduction-band minima for both materials of a heterostructure. The energies of the minima are determined by the tops of the valence bands, and the band gap, as well as by the change of the band gap, and shifts and splits in the energy of the bands under strain.

We assume the lattice constant in the heterojunction plane, $a_\parallel$, to be uniform along the heterostructure. In our work $a_\parallel$ corresponds to the lattice constant only for the (001) interface orientation. For the (111) interface orientation, $a_\parallel$ is equal to the distance between the nearest atoms in the growth plane multiplied by $\sqrt{2}$, and defines the unit-cell deformation in the heterojunction plane. We assume that $a_\parallel = 5.43$ Å in unstrained Si, and $a_\parallel = 5.65$ Å in unstrained Ge. The weighted averages of the valence bands (light-hole, heavy-hole, and spin-split-off bands) referred to those in Ge are determined by the following expressions:

$$E_{av}^{(111)} = (90.9a_\parallel - 1073.6)x \text{ meV} \tag{1}$$

$$E_{av}^{(001)} = (272.73a_\parallel - 1950.9)x \text{ meV} \tag{2}$$

for (111) and (001) interface orientation, respectively; $a_\parallel$ is expressed in Å. Formula (1) was derived by using the calculations from [4]. There are later theoretical works relating

to band offsets—for instance, [5, 10]. However, these calculations were carried out only for the (001) orientation of the heterointerface. Expression (2) was derived employing the results from [5]. In [5], one of the heterostructure materials was assumed to be unstrained. However, we extrapolated the results from [5] to the case of an arbitrary strain (that is, an arbitrary $a_\parallel$). Such extrapolation is partly justified by the following. The discontinuity in the weighted average of the valence bands varies linearly with the difference of the Si fraction in the materials of a heterostructure [4, 5], and the coefficient of proportionality depends only on $a_\parallel$ for all interface orientations [4]. The value (2) leads to underestimation of the valence-band offsets compared to the calculations in [4] for the (001) plane. For the Ge/Si heterostructures grown pseudomorphically on Si and Ge, the value of the valence-band discontinuity (2) differs from that in [4] by 70 and 100 meV, respectively. The valence-band offsets [4] are in better agreement with those [2] measured experimentally for the $Ge_{1-x}Si_x$ alloy ($0 < x < 0.3$) grown pseudomorphically on Ge, although the values [5] of the valence-band offsets fall within the limits of experimental error. On the other hand, the data [1] on the band gap of pseudomorphic $Ge_{1-x}Si_x$ ($0.76 < x < 1$) single layers on silicon are better described by [5], but the band gaps obtained employing the results in [5] and [4] differ from the experimental data by less than 2%.

The band gap for an unstrained $Ge_{1-x}Si_x$ alloy was investigated recently by Weber and Alonso [11]. For the differences in energy of the conduction-band minima at the L and Δ points and the top of the valence band (E_g^L and E_g^Δ, respectively), we use the analytical expressions from this paper ($T = 4.2$ K):

$$E_g^L = 740 + 1270x \text{ meV} \tag{3}$$

$$E_g^\Delta = 931 + 18x + 206x^2 \text{ meV}. \tag{4}$$

We assume these expressions to be valid for $0 < x < 1$. Such extrapolation is quite justified for (4), because formula (4) is derived from the experimental data for E_g^Δ which fall in the broad range of x ($0.15 < x < 1$). Recall that in unstrained $Ge_{1-x}Si_x$, for $x < 0.15$, the lowest conduction-band minima are at L points, but those for $x > 0.15$ occur at Δ points. The experimental data for E_g^L lie in a narrow composition range, and formula (3) can lead to a large error for x near 1.

To determine the strain splittings of the bands, and the variation of the energy gap, we use the theoretical values for the deformation potentials in Ge and Si from [4] for the (111) $Ge_{1-x}Si_x$/Ge heterostructure and from [5] for the (001) $Ge_{1-x}Si_x$/Si heterostructure. To find all of the required parameters for the alloy, we perform a linear interpolation between the values for the pure elements. For $a_\parallel$ for an unstrained alloy, we use the expression [13]

$$a_\parallel = 5.65 - 0.24x(1-x) - 0.22x^2 \text{ Å}.$$

The weighted averages of the L (Δ) minima are given by

$$E_{av}^{L,\Delta} = E_{av} + E_g^{L,\Delta} + \left(\Xi_d + \frac{1}{3}\Xi_u - a\right)^{L,\Delta} \mathrm{Sp}(\epsilon) + \frac{\Delta_{so}}{3} \tag{5}$$

where the third term describes the shift of the energy minima under homogeneous deformation [4], ϵ is the strain tensor, and Δ_{so} is the spin–orbit splitting.

2.1. The conduction band in (111) $Ge_{1-x}Si_x$/Ge heterostructures

Let us consider in some detail the conduction band in the $Ge_{1-x}Si_x$/Ge heterostructure. In this heterostructure for the (111) interface, a uniaxial strain splits the minima at L into two inequivalent groups: the band along [111] (we will denote it as the 1L valley), and the

other three bands (3L valleys). The minima at Δ remain degenerate. The energies of the L and Δ minima are determined by the expressions

$$E^{1L,3L} = E^{L}_{av} + \alpha^{1L,3L}\Xi^{L}_{u}\epsilon_{xy} \tag{6}$$

$$E^{\Delta} = E^{\Delta}_{av} \tag{7}$$

where $\alpha^{1L} = 2$ for the 1L valley, and $\alpha^{3L} = -2/3$ for the 3L valleys [4], and ϵ_{xy} is the strain tensor component.

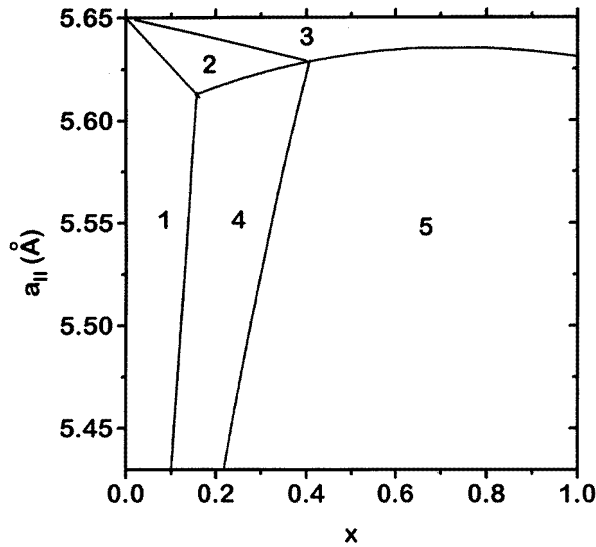

Figure 1. Regions of specific relative energy positions of the conduction-band-edge states in germanium and in the alloy for a (111) $Ge_{1-x}Si_x$/Ge heterostructure. At the bottom of the figure, the relative energy positions of the conduction-band edge in the germanium and the alloy are shown for all of the regions. Quantum confinement effects are not taken into account. $a_{\parallel}$ corresponds to the buffer layer on which a heterostructure is grown.

As mentioned above, the conduction-band minima in the Ge layer may lie at different points of the Brillouin zone, namely, at 1L, 3L, or Δ points. Furthermore, type-I or type-II band alignment may be realized.

Let us at first neglect the quantum confinement effects. For 5.43 Å $< a_{\parallel} <$ 5.65 Å, in the Ge layer the 3L valleys are not higher than the 1L valleys; moreover, the Δ valleys in the Ge layer are higher than those in the alloy layer. For simplicity, we consider only the lowest conduction-band minima in either layer for various values of $a_{\parallel}$ and x. Using

(6) and (7), we find the regions of fixed relative energy positions of the conduction-band-edge states in germanium and in the alloy for the (111) $Ge_{1-x}Si_x/Ge$ heterostructure (see figure 1). One can see from the figure that the conduction-band edge in Ge lies lowest in energy for the regions labelled 1, 2, and 4 (the type-I heterojunction), and highest for regions 3 and 5 (the type-II heterojunction).

We should remark that figure 1 is to be considered illustrative and qualitative, and merely demonstrates possible situations in the conduction band for various parameters of heterostructures. This lack of quantitative reliability may be attributed to errors in the energies of L minima (3), deformation potentials, and valence-band offsets (1). In addition, the strain in the layers may be quite sizeable (up to 4%)—such that, strictly speaking, nonlinearities are appreciable [12]. In this work we do not take these effects into account. Thus, in reality the regions of a specific conduction-band structure (in the implied meaning) can differ from those shown in figure 1. Moreover, it is quite possible that some regions depicted in figure 1 do not actually exist, and—vice versa—regions with a different structure of the conduction band may exist. Therefore, experimental examination of the conduction band is, of course, necessary.

In a Ge or alloy layer of finite width, the quantum confinement causes an increase in energy of the conduction-band minima. Consequently it makes the regions in figure 1 change and, in general, appear or disappear.

Employing results given by Van de Walle and Martin [4], and (3), it can be shown that the 1L valley in an alloy lies lower in energy than that in Ge for 5.43 Å $< a_\parallel <$ 5.65 Å and $0 < x < 1$. Therefore, although the $Ge_{1-x}Si_x/Ge$ heterostructure can have a direct band gap, here the potential wells for electrons and holes are at different layers (type-II confinement). This case is realized for region 3 in figure 1 in structures with thin $Ge_{1-x}Si_x$ layers.

2.2. The conduction band in (001) $Ge_{1-x}Si_x/Si$ heterostructures

In each layer of a $Ge_{1-x}Si_x/Si$ heterostructure grown on the (001) plane, the strain splits the Δ minima into four components along the [100], [$\bar{1}$00], [010], and [0$\bar{1}$0] directions (4Δ minima), and two components along [001] and [00$\bar{1}$] (2Δ minima). The four L points remain equivalent. The energies of the L and Δ minima are given by

$$E^L = E^L_{av} \tag{8}$$

$$E^{2\Delta,4\Delta} = E^{\Delta}_{av} + \alpha^{2\Delta,4\Delta}\,\Xi^{\Delta}_u(\epsilon_{zz} - \epsilon_{xx}) \tag{9}$$

where $\alpha^{2\Delta} = 2/3$ for 2Δ minima, and $\alpha^{4\Delta} = -1/3$ for 4Δ minima.

Figure 2 shows the relative energy positions of the conduction-band-edge states in layers of a $Ge_{1-x}Si_x/Si$ heterostructure for various values of $a_\parallel$ and x. Only the lowest valleys in each layer are pictured. The quantum confinement is not taken into account. For all of the regions in figure 2 except the fourth one, the lowest conduction-band minima in silicon are at 2Δ, and lie lower than in the alloy. Therefore, over a wide range of parameters, the band-edge optical transitions in the heterostructures with thin Si layers will be direct in quasi-momentum space. However, these transitions will be indirect in coordinate space, because, as mentioned above, the valence-band edge in the alloy layer lies highest in energy.

Employing tunnelling, one can reduce the separation of the electrons and holes by decreasing the width of either or both of the heterostructure layers. If this is done, the quantum confinement makes the regions in figure 2 change, and might cause them to appear or disappear. It should be remembered that quantum confinement in Si layers reduces the parameter regions for which $Ge_{1-x}Si_x/Si$ is a direct-gap structure. This is due to the fact

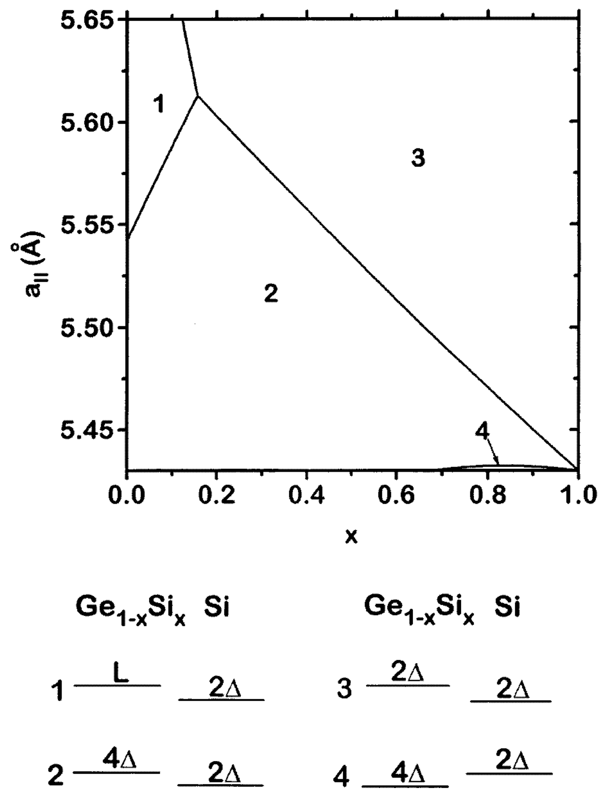

Figure 2. Regions of specific relative energy positions of the conduction-band-edge states in Si and in the alloy for a (001) $Ge_{1-x}Si_x/Si$ heterostructure. At the bottom of the figure, the relative energy positions of the conduction-band edge in Si and in the alloy are shown for all of the regions. Quantum confinement effects are not taken into account. $a_{\|}$ corresponds to the buffer layer on which a heterostructure is grown.

that the 2Δ minima in the alloy lie higher in energy than those in Si over the entire range of parameters considered (5.43 Å $< a_{\|} < 5.65$ Å, $0 < x < 1$), and the quantum confinement causes an increase in energy of the 2Δ minima in silicon. Thus, the 2Δ minima in a rather thin Si layer may be higher than some others. In contrast, decreasing the alloy width could just lead to growth of the parameter region over which the heterostructure has a direct band gap. That is, the quantum confinement in an alloy layer reduces region 4 in figure 2, and keeps it close up to the x-axis.

The approach given in [4] leads to very similar results: regions of the fixed conduction-band structure differ insignificantly from those in figure 2. In particular, the region corresponding to the fourth region in figure 2 is slightly bigger, and extends from $x \approx 0.6$ to $x = 1$.

Let us compare the results which have been obtained by employing the results from [5], and (4), with some experimental data for $Ge_{1-x}Si_x$ layers grown pseudomorphically on unstrained Si. The energy differences between the lowest conduction-band edge and the top of the valence bands in the alloy, as noted above, agree within 2% (to better than $\approx$13 meV) with the expression valid for $x > 0.76$, which was experimentally obtained in [1]. The energy difference between the Δ minima in Si and the 4Δ minima in the alloy,

ΔE_c, is less than 8 meV for region 4 in figure 2. This fact agrees with [1], where the conduction-band offset, $|\Delta E_c|$, was shown to be less than 10 meV for the $Ge_{0.17}Si_{0.83}/Si$ heterostructure. Although the discrepancy between the theoretical [5] and experimental [1] values of the band gap is relatively small, it is still more than the conduction-band offset $|\Delta E_c|$. Thus the question of the real existence of type-I band alignment is still open. As far as we are aware, this problem has not yet been solved experimentally, either: for $x > 0.64$ there is experimental evidence which is more readily explained for a type-I [1, 6] or type-II [7] band alignment. In the following sections, we will discuss the problem of specifying the type of the lowest conduction-band minima, as well as the type of band alignment.

3. Selection rules for optical transitions in (111) $Ge_{1-x}Si_x/Ge$ heterostructures

In the previous section, we have shown that the conduction-band bottoms in the $Ge_{1-x}Si_x/Ge$ heterostructure can be in 3L, 1L, or Δ valleys. In this section the selection rules for the dipole indirect optical transitions between the valleys and the valence band are considered. Because of the strain ($a_\parallel < 5.65$) and the quantum confinement effect, the top of the valence band is formed from the heavy-hole states with large mass in the [111] direction. Therefore, we consider transitions only in or from these states. Note that if the lattice constant $a_\parallel$ is larger than that in an unstrained alloy, then in very thin Ge layers (width less than 10–20 Å), the top of the valence bands can be formed from the light-hole states. This is possible only for the above deformations, because in this case the top of the heavy-hole subband is lower than the top of the light-hole subband in the alloy.

We consider a QW structure with a symmetry plane at the centre of a quantum well. The groups of the wave vector at different points of the Brillouin zone, and the irreducible representations for the corresponding electron and hole wave functions are shown in table 1(a). Representations of the momentum operator components and those of the phonon wave functions are shown in the same table. We use common notation for the phonons: the letters L, T for longitudinal and transverse phonons, and O, A for optical and acoustical phonons.

3.1. hh–1L transitions

By using a standard method [14, 15], we find the following selection rules for optical phonon-assisted transitions between the heavy-hole subband and the 1L valley. Similarly to the case for bulk germanium, the LO- and TA-phonon-assisted transitions are forbidden because of parity conservation. TO-phonon-assisted transitions are allowed for any light polarization. LA-phonon-assisted transitions are allowed only for photons which have nonzero electric field components $\boldsymbol{E}$ on the (111) plane.

As we noted above, a direct-gap structure may be realized if the conduction-band bottom is in the 1L valley. But the direct dipole optical transitions from heavy-hole and light-hole subbands in 1L valleys are forbidden. The problem is that the electron and hole wave functions have even parity (this is denoted by the superscript $+$ in the representation notation), but dipole transitions are forbidden between same-parity states. This assertion is not valid for transitions with a change in the level number—for example, for transitions between the second hole subband and the first 1L valley (electron) subband. This is due to the odd parity of wave functions in even subbands. Thus the wave function representations in even subbands are L_6^- and $L_4^- + L_5^-$ for the electron and hole, respectively. Note that in this case the LO- and TA-phonon-assisted transitions are allowed, too.

It can be proved that the hh–1L LA-phonon-assisted transition is forbidden for $\boldsymbol{E} \parallel [111]$ in an asymmetric heterostructure.

Table 1. (a) Wave-vector groups at different points of the Brillouin zone, and irreducible representations for electron and hole wave functions, phonons, and operator momentum components for a (111) $Ge_{1-x}Si_x/Ge$ structure. A normal direction to the growth plane is labelled z; two directions in the growth plane are labelled x and y. We use the notation for irreducible representations for the D_{3d} and C_{4v} groups from [14], for the C_{2v}, C_{2h}, and σ-groups we use that from tables 2–4, and for the D_{4h} group we use that from [18] and table 5. (b) As (a), but for the (001) $Ge_{1-x}Si_x/Si$ structure.

(a)			Irreducible representation	Group
Heavy holes			$L_4^+ + L_5^+$	D_{3d}
Light holes			L_6^+	
p_z			L_1'	
p_x, p_y			L_3'	
1L valley	Electrons		L_6^+	
	Phonons	LA	L_2^-	
		LO	L_1^+	
		TA	L_3^+	
		TO	L_3^-	
3L valley	Electrons		$B_1^+ + B_2^+$	C_{2h}
	Phonons	LA	A_1^-	
		LO	A_1^+	
		TA	$A_1^+ + A_2^+$	
		TO	$A_1^- + A_2^-$	
p_z			A_2^-	
p_x, p_y			A_1^-	
Δ valley	Electrons		$B_1 + B_2$	σ
	Phonons	LA	A_1	
		LO	A_1	
		TA	A_2	
		TO	A_2	
p_z			A_1	
p_x, p_y			A_2	

3.2. hh–3L transitions

The dipole hh–3L transitions are allowed for any light polarization, if assisted by LA and TO phonons, and are forbidden for other phonons.

Thus, for photons with $\boldsymbol{E} \parallel [111]$, the hh–3L LA-phonon-assisted transitions are allowed, and the hh–1L transitions are forbidden. It is interesting to find the intermediate states for allowed transitions. It turns out that allowed transitions are realized through $L_4^- + L_5^-$ and $B_1^- + B_2^-$ states. The intermediate $L_4^- + L_5^-$ state arises from the Γ_8^- conduction-band state of bulk Ge, and the $B_1^- + B_2^-$ state arises from the $L_5^- + L_4^-$ valence-band state. It is more probable that transitions are through the $B_1^- + B_2^-$ state, because it is nearest to the initial valence-band state. In bulk Ge, optical LA-phonon-assisted transitions are realized through the intermediate state in the Γ_7^- conduction band [16]. In a heterostructure, the same transitions are realized through the L_6^- state which arises from Γ_7^-. These transitions are caused only by the electrical field components located in the (111) plane. The energy

Table 1. (Continued)

(b)			Irreducible representation	Group
Heavy holes			$E_1'^{+}$	D_{4h}
Light holes			$E_2'^{+}$	
p_z			A_2^-	
p_x, p_y			E^-	
2Δ valley	Electrons		Δ_6	C_{4v}
	Phonons	LA	Δ_1	
		LO	Δ_2'	
		TA	Δ_5	
		TO	Δ_5	
p_z			Δ_1	
p_x, p_y			Δ_5	
4Δ valley	Electrons		E'	C_{2v}
	Phonons	LA	A_1	
		LO	A_2	
		TA	$B_1 + B_2$	
		TO	$B_1 + B_2$	
p_z			A_1	
p_x, p_y			B_1, B_2	

Table 2. Characters of the irreducible representations for the double C_{2h} group. The notation for the group elements is taken from [18].

C'_{2h}	E	Q	C_2	QC_2	σ	$Q\sigma$	I	QI
A_1^+	1	1	1	1	1	1	1	1
A_2^+	1	1	−1	−1	−1	−1	1	1
A_1^-	1	1	1	1	−1	−1	−1	−1
A_2^-	1	1	−1	−1	1	1	−1	−1
B_1^+	1	−1	i	−i	i	−i	1	−1
B_2^+	1	−1	−i	i	−i	i	1	−1
B_1^-	1	−1	i	−i	−i	i	−1	1
B_2^-	1	−1	−i	i	i	−i	−1	1

difference between the initial and intermediate states is less for transitions through the L_6^- state than for transitions through the $B_1^- + B_2^-$ state; therefore, the probability of the hh–3L transition through the L_6^- state is higher. This means that the probability of the LA-phonon-assisted hh–3L transition caused by $\boldsymbol{E} \parallel [111]$ is less than that of the one caused by $\boldsymbol{E} \perp [111]$.

3.3. hh–Δ transitions

Symmetry allows any hh–Δ phonon-assisted optical transition for any light polarization. Yet, in bulk Si and in bulk $Ge_{1-x}Si_x$ alloy, only TA- and TO-phonon-assisted transitions

Table 3. The irreducible representation characters of the double σ-group. The notation for the group elements is taken from [18].

σ'	E	Q	σ	$Q\sigma$
A_1	1	1	1	1
A_2	1	1	−1	−1
B_1	1	−1	i	−i
B_2	1	−1	−i	i

Table 4. The irreducible representation characters of the double C_{2v} group. σ_{1v} and σ_{2v} denote symmetry planes crossing the C_2 axis.

C'_{2v}	E	Q	C_2, QC_2	σ_{1v}, $Q\sigma_{1v}$	σ_{2v}, $Q\sigma_{2v}$
A_1	1	1	1	1	1
A_2	1	1	1	−1	−1
B_1	1	1	−1	1	−1
B_2	1	1	−1	−1	1
E'	2	−2	0	0	0

Table 5. The irreducible representation characters of the double D_{4h} group. u and u' denote twofold rotation axes which are perpendicular to the fourfold rotation axis C_4.

D'_{4h}	E	Q	C_2, QC_2	C_4, C_4^{-1}	QC_4, QC_4^{-1}	$2u$, $2Qu$	$2u'$, $2Qu'$
$E_1'^+$	2	−2	0	$\sqrt{2}$	$-\sqrt{2}$	0	0
$E_2'^+$	2	−2	0	$-\sqrt{2}$	$\sqrt{2}$	0	0
$E_1'^-$	2	−2	0	$\sqrt{2}$	$-\sqrt{2}$	0	0
$E_2'^-$	2	−2	0	$-\sqrt{2}$	$\sqrt{2}$	0	0
D'_{4h}	I	QI	IC_2, QIC_2	IC_4, IC_4^{-1}	QIC_4, QIC_4^{-1}	$2Iu$, $2QIu$	$2Iu'$, $2QIu'$
$E_1'^+$	2	−2	0	$\sqrt{2}$	$-\sqrt{2}$	0	0
$E_2'^+$	2	−2	0	$-\sqrt{2}$	$\sqrt{2}$	0	0
$E_1'^-$	−2	2	0	$-\sqrt{2}$	$\sqrt{2}$	0	0
$E_2'^-$	−2	2	0	$\sqrt{2}$	$-\sqrt{2}$	0	0

between the valence band and the Δ valleys are observed [1, 11]. Symmetry does not account for the absence of longitudinal-phonon-assisted transitions [15]; therefore, in the heterostructure $Ge_{1-x}Si_x$/Ge, only transverse-phonon-assisted transitions can be observed.

In summary, we now briefly formulate the selection rules for phonon-assisted optical transitions between the valence band and different conduction-band valleys in a $Ge_{1-x}Si_x$/Ge heterostructure grown on a (111) plane. If the conduction-band minima are at Δ, then the TO-phonon-assisted optical transitions are predominant [1]. When the conduction-band minima are at any L points, LA-phonon-assisted optical transitions prevail [17]. LA-phonon-assisted transitions from 1L and 3L valleys differ in polarization. LA-phonon-assisted transitions with $\boldsymbol{E} \parallel [111]$ are forbidden for the 1L valley, and are reduced for 3L valleys.

4. Selection rules for optical transitions in (001) $Ge_{1-x}Si_x/Si$ heterostructures

Again, we consider a QW heterostructure with the symmetry plane in the centre of a quantum well. The notation for the wave-vector groups and irreducible representations is shown in table 1(b). As we noted, the top of the valence band lies highest in the layer with the largest Ge fraction (in this case, in the alloy layer). In the alloy layer, the relative positioning of the valence-band tops for heavy and light holes depends on a lattice constant, $a_{\parallel}$. If $a_{\parallel}$ is less than that in an unstrained alloy, then the top of the heavy-hole band is higher, while, in contrast, the top of the light-hole band is higher for the reverse relationship between the lattice constants (if quantum confinement is neglected). This has to be taken into account in the selection rule analysis.

As shown in figure 2, the conduction-band bottoms may be in 2Δ or 4Δ valleys. The phonon-assisted transitions from 4Δ valleys to light-hole and heavy-hole subbands are allowed for any phonon and any light polarization.

The transverse-phonon-assisted transitions from 2Δ valleys to light-hole and heavy-hole subbands are allowed for any light polarization. The longitudinal-phonon-assisted transitions to light/heavy hole subbands are allowed for $\boldsymbol{E} \perp [001]$. In the case where $\boldsymbol{E} \parallel [001]$, the LA-phonon-assisted transitions between 2Δ valleys and a light-hole band are forbidden, but the transitions between 2Δ valleys and a heavy-hole subband are allowed. In contrast, the LO-phonon-assisted transitions to a light-hole subband are allowed, and transitions to a heavy-hole band are forbidden. Longitudinal-phonon-assisted transitions are not observed in Si and the alloy. Therefore, in the study of optical transitions, one cannot distinguish between those from 4Δ valleys and those from 2Δ valleys.

Unlike the transitions from 4Δ valleys, transitions from 2Δ valleys can be realized without scattering. They are direct in momentum space and indirect in coordinate space. Symmetry allows these transitions to light-hole and heavy-hole subbands, if the electrical field vector has nonzero components in the (001) plane. For $\boldsymbol{E} \perp (001)$, transitions to the light-hole subband are allowed, but transitions to the heavy-hole subband are forbidden.

The direct transition intensity must rise with decreasing layer thickness, because of the greater overlap of wave functions in the coordinate and momentum spaces. In contrast, the zero-phonon transition intensity from the 4Δ valleys (region 4 in figure 2) depends weakly on Si and the alloy layer thickness, given a good quality of heterointerfaces. Therefore, one can distinguish between the transitions from 4Δ and 2Δ valleys by investigating the dependency of the ratio of the phonon-assisted-line intensity to the zero-phonon-line intensity on the layer thickness.

Certainly, there are more direct methods for identification of the type of the lowest valley in a conduction band. For example, this may be done by making cyclotron resonance measurements of the electron masses. However, these measurements require a very high quality of structure. The requirements for structure quality allowing observation of optical phenomena may be less stringent, and, consequently, the methods suggested here can be easier.

Acknowledgments

We are grateful to Professor Yu A Romanov for fruitful discussions, continuing encouragement, and support. This work was partly supported by the Russian Foundation for Basic Research (grants 95-02-05863 and 96-02-16991), and by INTAS (grant 94-842).

References

[1] Robbins D J, Canham L T, Barnet S J, Pitt A D and Calcott P 1992 *J. Appl. Phys.* **71** 1407
[2] Yaguchi H, Tay K, Takemasa K, Onabe K, Ito R and Shiraki Y 1994 *Phys. Rev.* B **49** 7394
[3] Orlov L K, Kuznetsov O A, Rubtsova R A, Chernov A L, Gavrilenko V I, Mironov O A, Nikanorov V V, Skrylev I Yu and Chystyakov S V 1990 *Sov. Phys.–JETP* **98** 1028
[4] Van de Walle C G and Martin R M 1986 *Phys. Rev.* B **34** 5621
[5] Rieger M M and Vogl V 1993 *Phys. Rev.* B **48** 14 276
[6] Glaser E, Trombetta J M, Kennedy T A, Prokes S M, Glembocki O J, Wang K L and Chern C H 1990 *Phys. Rev. Lett.* **65** 1247
Glaser E R, Kennedy T A, Godbey D J, Thompson P E, Wang K L and Chern C H 1993 *Phys. Rev.* B **47** 1305
Northrop G A, Morar J F, Wolford D J and Bradley J A 1992 *J. Vac. Sci. Technol.* B **10** 2018
Fukatsu S and Shiraki Y 1993 *Appl. Phys. Lett.* **63** 2378
[7] Baier T, Mantz U, Tronke K and Sauer R 1994 *Phys. Rev.* B **50** 15 191
[8] Pearsall T P, Berk J, Feldman L C, Bonar J M and Mannaerts J P 1987 *Phys. Rev. Lett.* **58** 729
[9] Gnutzmann U and Clausecker K 1974 *Appl. Phys.* **3** 9
[10] Colombo L, Resta R and Baroni S 1991 *Phys. Rev.* B **44** 5572
[11] Weber J and Alonso M I 1989 *Phys. Rev.* B **40** 5683
[12] Ma Q M, Wang K L and Schulman J N 1993 *Phys. Rev.* B **47** 1936
[13] Dismukes J P, Ekstrom L and Paff R J 1964 *J. Phys. Chem.* **68** 3021
[14] Bassani F and Pastori Parravicini G 1975 *Electronic States and Optical Transitions in Solids* (Oxford: Pergamon)
[15] Knox R S and Gold A 1964 *Symmetry in the Solid State* (New York: Benjamin)
[16] Bir G L and Pikus G E 1974 *Symmetry and Strain-Induced Effects in Semiconductors* (New York: Wiley)
[17] Kalugin N G, Orlov L K and Kuznetsov O A 1993 *Sov. Phys.–JETP* **58** 200
[18] Landau L D and Lifshitz E M 1974 *Quantum Mechanics* (Oxford: Pergamon)